Experimental measurement of soil-intruder interactions for soft robots design

Bachelor Thesis by

Ahmet Tekin

S2727196

University of Twente

Supervisors:

Floriana Anselmucci

Ilya Brodoline

28-06-2024

Summary

In this thesis, an adaptation of Cone Penetration Testing CPT is done to find the most efficient tip shape to penetrate in sand. Additionally, a setup is proposed for cavity expansion testing, which should examine expandable chambers in sand. These tests should be used to create a database to ultimately improve the design of the soil-intruding robot. The results of the penetration tests are quite interesting. It is found that the smaller the contact area between the tip and the sand is, the lower the penetration resistance is. This is seen in tip SD (Small Diameter) and AR4 (Aspect Ratio 4). As long as the tip AR4 has not reach base diameter of the body (30 mm), there is a relatively small penetration resistance. Furthermore, there is a strong relation in vertical penetration testing between the aspect ratio and the penetration resistance. AR4 requires the least amount of force to penetrate, followed by AR2.5 and finally AR1. The asymmetric tip performs worst in vertical penetration tests, along with AR1. However, that is not the case in horizontal penetration tests. The asymmetric tip with the beak facing up or down performs best in low depths. There is a clear difference between the beak facing to side, since the penetration resistance is highest among the orientations of the asymmetric tip.

Contents

1. Introduction

In a search for sustainable and resilient infrastructural development, the dynamic interaction between technology and the earth's underground environments grows as a critical frontier of research. The stability and longevity of man-made structures are dependent on the underground world that comes with a variety of soil types and characteristics. This underground environment is constantly changing due to the dynamics of the climate, making the structure of soil vulnerable to drastic and unpredictable changes (Meurer et al., 2020). These changes carry great risk, endangering the structural integrity of vital structures.

The traditional methodologies used for underground exploration and monitoring, while useful, do not comply with the current adaptation of climate change and sustainability (Huang et al., 2022). In response to this, the development of more sustainable soil monitoring have begun. This is done by looking at nature, as the development of a soil-burrowing robot is inspired from earth's burrowing animals, in particular an earthworm. This offers an innovative approach for exploring below the surface. These robots mimic the natural ability of animals to penetrate and navigate through soil efficiently, incorporating mechanisms that allow them to anchor themselves within the ground and penetrate the soil to advance (Chowdhury et al., 2017). Because they can move through the ground with little difficulty, soil-burrowing soft robots present a viable option for carrying out soil research, such as soil sampling or monitoring moisture levels.

Although these soil-burrowing soft robots have promising capabilities, however the flaws such as their inability to dig deep into soil limit their practical applicability. To overcome this challenge, a thorough comprehension of the soil-robot interaction is required. Understanding the interactions between the penetration and anchoring of the robot and the soil is part of that challenge. This thesis focuses on building a data base for those interactions through experiments.

2. Problem Context

2.1. Problem Statement

An important development in the search for sustainable and non-intrusive underground exploration methods is the development of soil-burrowing soft robotics, which gets inspiration from the peristaltic movement of earthworms. These soft robots, which minimize environmental disturbance and provide access to small places underground other mechanisms cannot reach (Omori et al., 2009), can completely transform the approach to soil investigation. However, an important challenge to the actual implementation of this technology is the incomplete knowledge of the complex relationships between penetrating tip and expandable chamber and the soil, as the current robotic probe cannot dig deep into the soil yet. A robotic earthworm can roughly dig 40 cm into the ground (Isaka et al., 2019), which is quite an accomplishment, but there is definitely still room for improvement.

Current numerical methods, such as Finite Element Method (FEM) have made progress in simulating soil-robot interactions (Dang & Meguid, 2011). However, they often fall short of capturing the full complexity of real-world conditions, mainly because of the wide variety of soil types and the changes of soil properties under different environmental conditions. Additionally, simulation of the robotic probe in the soil follow theoretical rules, which often cannot be replicated with theoretical hypotheses.

The lack of a comprehensive database on soil properties makes it more difficult for engineers to predict and improve the performance of soil-intruding robots. Key soil parameters such as shear strength and cohesion are crucial for designing soft robots that can go underground effectively and adaptively. Without this important knowledge, designing soft robots that can go underground effectively and adaptively remains a difficult task, restricting the variety of applications for soil-intruding robots in civil engineering.

2.2. Research Objective

The primary objective of this research is to develop a comprehensive database of soil properties through experimental measurements. This database will contain critical characteristics of soil, such as shear resistance and the relationship between pressure exerted onto the soil and radial displacement during soil deformation. These properties are derived from measurements taken during Cone Penetration Testing (CPT) and cavity expansion tests. CPT primarily measures

cone resistance, this resistance can be converted to indicate the shear resistance of the soil, providing valuable insights into its strength under stress. Similarly, measurements from cavity expansion tests reveal how soil expands radially under pressure. The experiments are designed to explain the interactions between soil properties and intruding equipment, simulating the conditions encountered by soil-burrowing soft robots' peristaltic movement.

3. Theory

3.1. Peristaltic Movement

The design of the robotic probe is inspired by the peristaltic motion of an earthworm, utilizing a series of contractions and relaxations along its body to move through soil. Whilst the shortened segment anchors to the soil, the lengthened segment advances the body along the trajectory, this can be seen in Figure 1. A segment will expand as it contracts longitudinally, increasing the frictional locking action with its surroundings. The opposing forces produced by the clamping action enable the remaining segments to extend longitudinally and move the earthworm's body forward (Winstone et al., 2016).

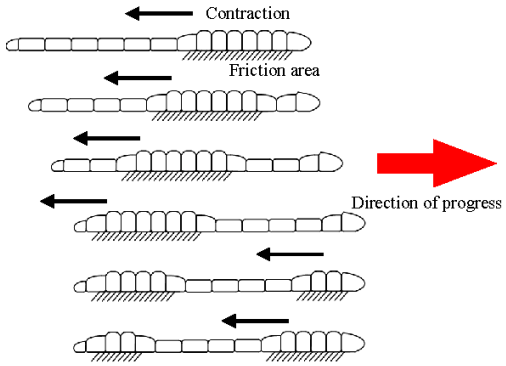

Figure 1: Peristaltic Movement of an Earthworm (Chowdhury et al., 2017)

Figure 2 illustrates how the robotic probe designed by University of Twente will accomplish this. It functions by having one section that can alter length longitudinally and two chambers that can grow radially, providing the anchoring. The robotic probe is connected to a pneumatic pump through three tubes, in order to control the expansion and contraction of each chamber. However, in the most recent prototype, the tubes are connected to a hydraulic pump instead of a pneumatic pump.

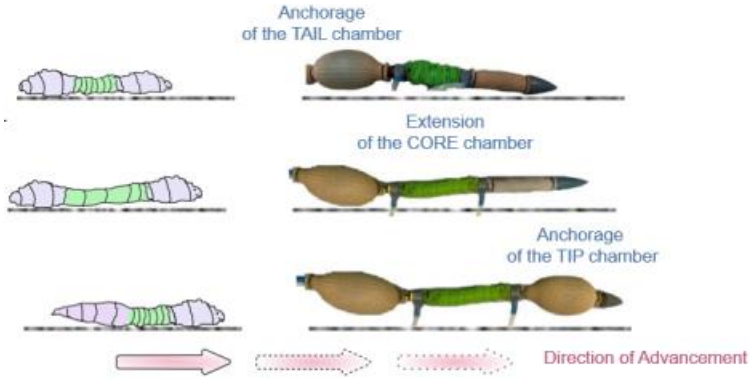

Figure 2: Mechanics of Peristaltic Locomotion of Robotic Probe

As can be seen from Figure 2, the ending chamber of the robotic probe can radially expand giving the anchorage to the body, and the core chamber expands longitudinally, giving the advancement of the body. The experiments done in this thesis are the Cone Penetration Test (CPT) and the cavity expansion test, since these mimic the two parts of the peristaltic locomotion of the robotic probe. Through the CPT, data will be collected to better understand the penetrating part of the robotic probe's locomotion in the soil. Better understanding the anchoring of the robotic probe is done through the cavity expansion test.

4. Cone Penetration Test

Cone penetration testing (CPT) is a method used in geotechnical engineering to determine the geotechnical properties of soils. It involves the penetration of a cone into the ground at a constant rate. This test provides continuous readings of the cone resistance, sleeve friction, and pore water pressure, which are used to determine soil characteristics (Mayne, 2007).

For this thesis, an adaptation of CPT is used to collect data on the interactions with the hard tip of the soil-intruding robot and the soil. The cone is replaced by a tip that mimics the tip of the robot. The main parameters that are looked at during this test are the penetration resistance and the penetration advancement. This gives insight to how much power is needed for the tip to advance into the soil, and with that ultimately the soil-intruding robot. The penetration advancement is done vertically and horizontally, since there is an expected difference in the stress pattern between these.

4.1. Methodology

Both the vertical and horizontal penetration tests are based on the same premises. The procedure begins with the positioning of the penetrometer at the surface of the prepared soil sample. The penetrometer will record data continuously as it advances into the soil, making an accurate assessment of soil resistance. A typical scheme for a penetrometer can be seen in Figure 3.

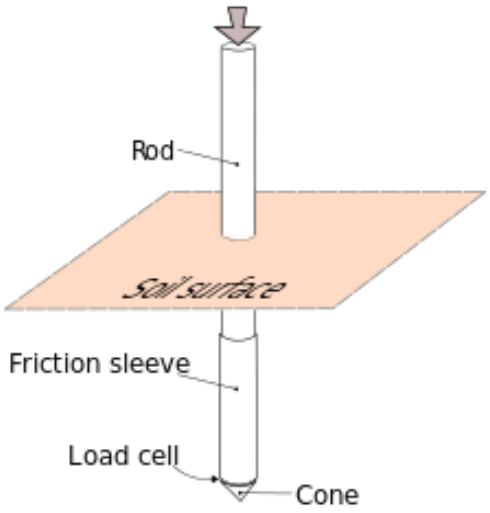

Figure 3: Typical scheme of Penetrometer (Lusilier, 2013)

The penetrometer is driven by a stepper motor connected to a threaded rod. The stepper motor makes the threaded rod spin, which ultimately causes the penetrometer to go down. This is visualized in Figure 4.

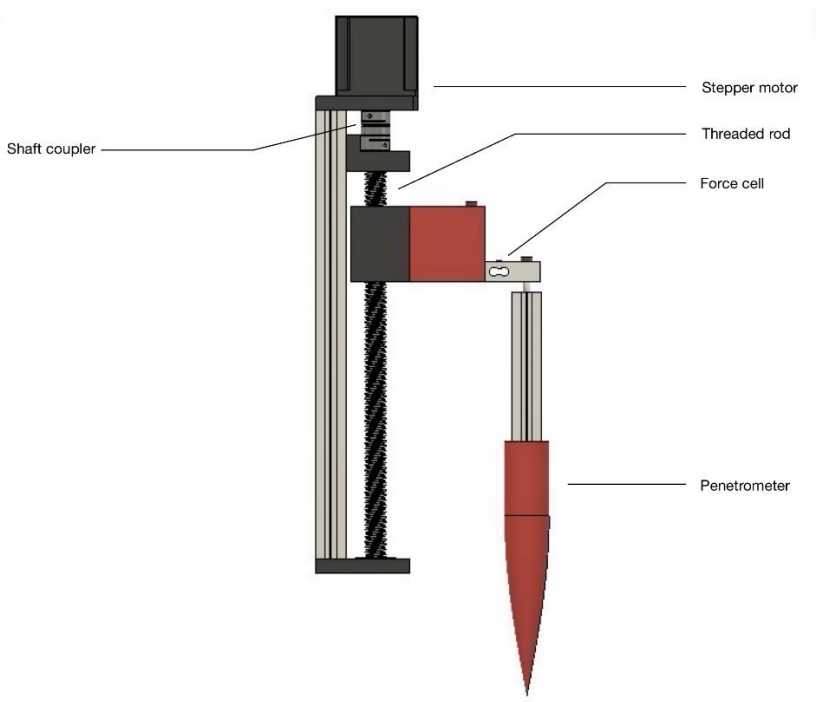

Figure 4: CPT setup side view

The stepper motor and force cell are both connected to an Arduino. The force cell has 2 strain gauges on it which measure the force needed to advance and sends this information to the Arduino, which is connected to a PC. The stepper motor is programmed to turn at a constant rate. For every full rotation created by the stepper motor, the penetrometer advances 5 mm. The measured penetration resistance [N], along with the penetration advancement [mm] is visualized and saved to a csv file using Serialplot software.

The penetrometer seen in Figure 4 is just one of the six tip bodies that are used in the experiment. All the bodies can be seen in Figure 5.

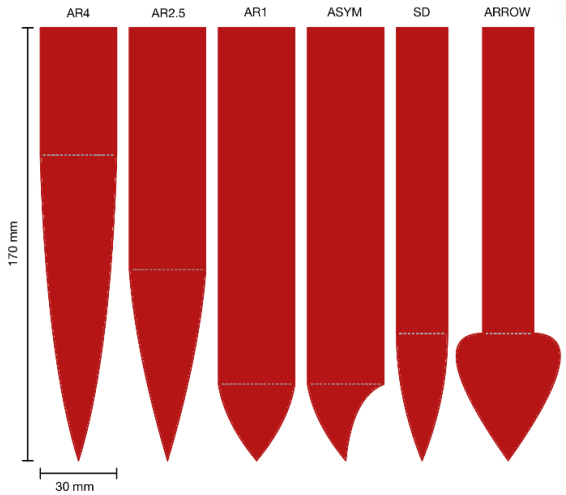

Figure 5: All bodies used for penetration tests

All bodies have a length of 17 cm and most of them have a diameter of 30 mm. The bodies are named ARx, ASYM, SD, or ARROW. AR stands for aspect ratio. The number that follows is the ratio between the tip length and the diameter. ASYM is a body with an asymmetric tip, inspired by the beak of a sandfish skink. SD stands for small diameter, this body has a diameter of 20 mm and has an aspect ratio of 2.5.

The soil used for the tests is dry sand. The tests will also be performed in different densities. The densities are achieved by tapping the sides of the container filled with sand with a hammer to compress the sand. Additional sand is then added on top and the sides of the container will be tapped lightly again until the wanted density is achieved. The sand is a mixture of sand particles that are smaller than 2 mm with a D_{50} value of roughly 0.8. The densities used in the tests are: 1.42 g/cm^3, 1.48 g/cm^3, 1.54 g/cm^3, 1.60 g/cm^3, and 1.66 g/cm^3.

Lastly, multiple penetration rates are tested. The rates differ as a result of the stepper motor doing more rotations in a certain time. This can simply be programmed.

All experiments with a certain set of parameters are done at least three times. This is done since not every run will lead to the same result. Doing more runs will ultimately give a range that is more reliable than a single run.

4.1.1. Vertical Penetration Test

In the vertical rigid penetration test, the device seen in Figure 4 is placed on top of a cylindrical container filled with sand. The setup can be seen in Figure 6 below.

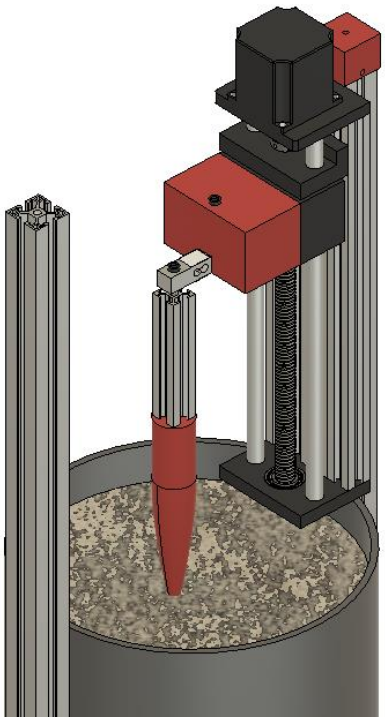

Figure 6: Vertical rigid penetration test setup

The cylindrical container has a diameter 24 cm and a height of 75 cm. As mentioned before, each combination of parameters is done at least three times. Each run, the sand is drained out of the container and put in again. This is to avoid pre-sheared conditions of the sand. The test starts with the tip being submerged a couple of millimetres in the sand, and proceeds to penetrate the sand 20 cm deep. The penetration will stop prematurely if the maximum force of 385 N is reached. This is done to avoid the setup from breaking or bending too much.

In the vertical rigid penetration test , all tip geometries are used. These are; AR1, AR2.5, AR4, ASYM, SD, and ARROW. These are each tested in five different densities; 1.42 g/cm^3, 1.48 g/cm^3, 1.54 g/cm^3, 1.60 g/cm^3, and 1.66 g/cm^3. Finally, three different penetration rates are tested on a certain selection of tip shapes; 0.25 turn/s, 0.5 turn/s, and 1 turn/s. With a conversion rate of 5 mm/turn, the penetration rates are 1.25 mm/s, 2.5 mm/s, and 5 mm/s respectively. In case not all penetration rates are tested, the default value of 0.5 turn/s is used.

To sum up, in the vertical penetration tests, the measured results are:

- Penetration resistance (q_c): The resistance against the tip as it penetrates the soil.
- Penetration advancement (d): The length the penetrometer advances into the soil.

The parameters are:

- Tip geometry

- Soil density
- Penetration rate

4.1.2. Horizontal Penetration Test

In the horizontal penetration tests, the device seen in Figure 4 is mounted on an aluminium structure that allows for easy movement of the device. This is needed to position the device correctly for different holes in the tank. That is because the sand for horizontal CPT in a relatively large wooden tank. The tank has several holes along the height of the tank. The holes in the tank allow for penetration tests to be conducted at different depths. This is done to evaluate the effect of static stress on horizontal penetration. The wooden tank along with its dimensions can be found in Figure 7 below.

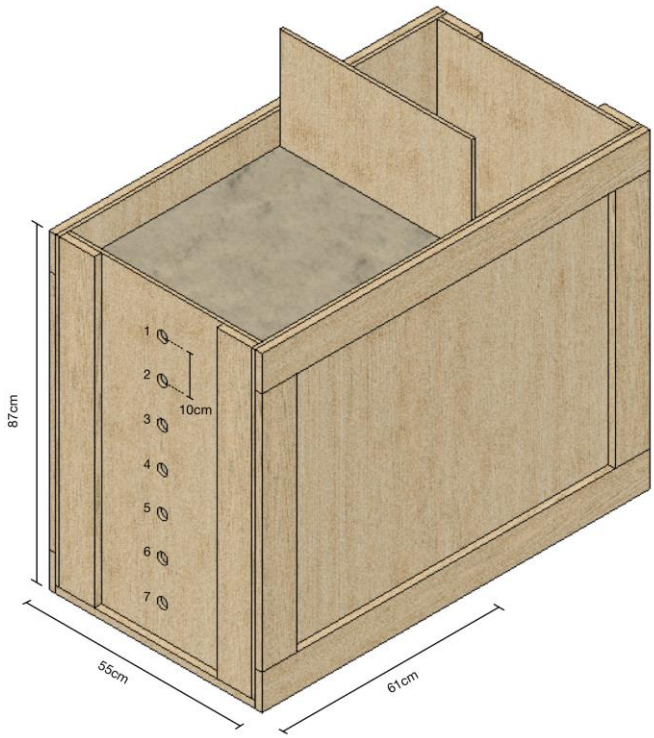

Figure 7: Wooden tank filled with sand

The tests are done on multiple holes, that each have 10 cm in between them. This translates to an increase of roughly $\sigma = \gamma \times z = 1.57N/cm^3 \times 10cm = 15.7N/cm^2$ per hole. As mentioned earlier, to position the device correctly, an aluminium structure is installed, where the device can be mounted to position in the front plane of the tank. The reason the structure allows for horizontal movement is that the holes are not perfectly aligned. The structure along the device can be seen in Figure 8 below.

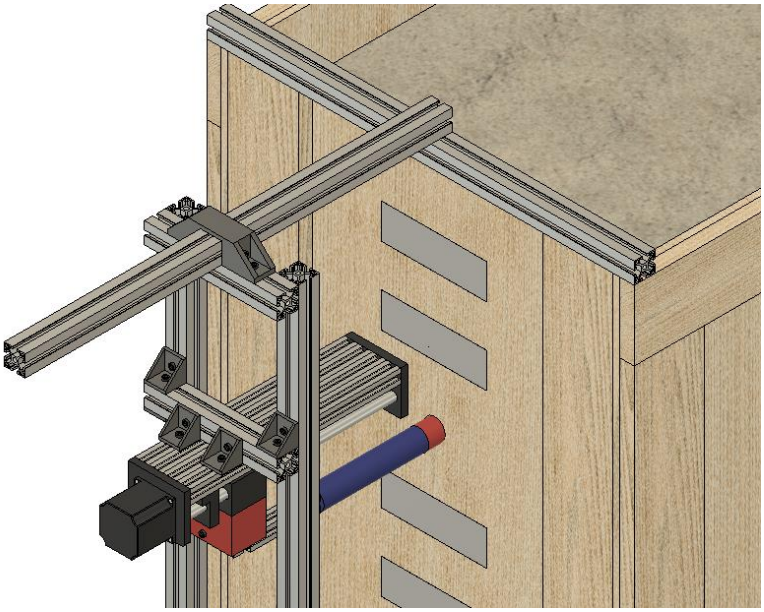

Figure 8: Horizontal CPT setup

As seen in Figure 8 by the connections on the aluminum frame, the device can be moved towards and away from the tank as well. This is to allow easy change of tip bodies. After the structure is put in place in a way where the body goes through to the hole perpendicularly, it should be mounted securely in place. This avoids the structure moving backwards when forces get high, and minimizes bending. However, it is important to note that all tests that cover the same depth should be performed after one another without adjusting the position of the device in the meantime.

Unlike the vertical rigid penetration tests, the tests cannot be performed from the absolute tip of the body. Doing this would allow sand to fall out of the hole that is being penetrated since the absolute tip of the body has a smaller diameter than the hole. To avoid sand falling out the hole, it should at all times be covered with the body of the tip that has a diameter of 30 mm. This is possible with the introduction of an extension piece which essentially lengthens the body. The extension piece has a diameter equal to the diameter of the hole and the base of the body, therefore no sand with fall out. As a result, the penetrating body is already fully submerged in the sand when it starts the run. Thus the starting point is 17 cm into the tank. This can be seen in Figure 9, along with the position of the extension piece, seen in blue.

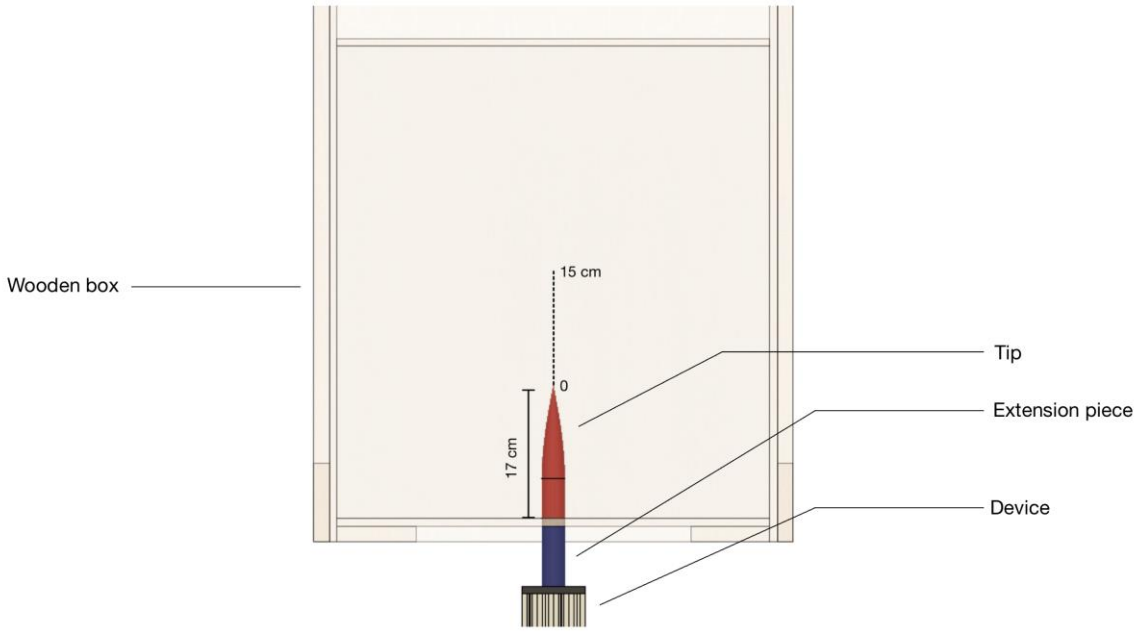

Figure 9: Top view of horizontal CPT showing penetration path

As can be seen from the figure, the blue extension piece is outside of the box and goes through the hole just enough for the red body to be at the beginning of the box. Since the extension piece is 15 cm long, the entire penetration is 15 cm as well (or shorter if maximum force of 350 N is reached), indicated by the dotted line in Figure 9. Penetrating further than 15 cm will cause sand to fall out the tank again, and alter the results. To prevent sand falling out during the experiment from other holes, they should be covered. This is done using a plug held in place by a piece of tape over the holes, see Figure 8.

In horizontal CPT, four tip geometries are used; AR1, AR2.5, AR4, and ASYM. The density of the sand is 1.57 g/cm^3. The second through fourth hole from up are used to see the difference that static stress creates, these can be seen in Figure 7 indicated by their number. These are 12 cm, 22 cm, and 32 cm deep. That translates to 18.8 N/cm^2, 34.5 N/cm^2, and 50.2 N/cm^2 respectively. All tests are done with a penetration rate of 0.5 mm/turn, which is 2.5 mm/s.

Additionally, since the asymmetric tip is expected to perform well due to its shape inspired by the beak of a sandfish skink, multiple orientations are tested. The orientations that are tested can be seen in Figure 10.

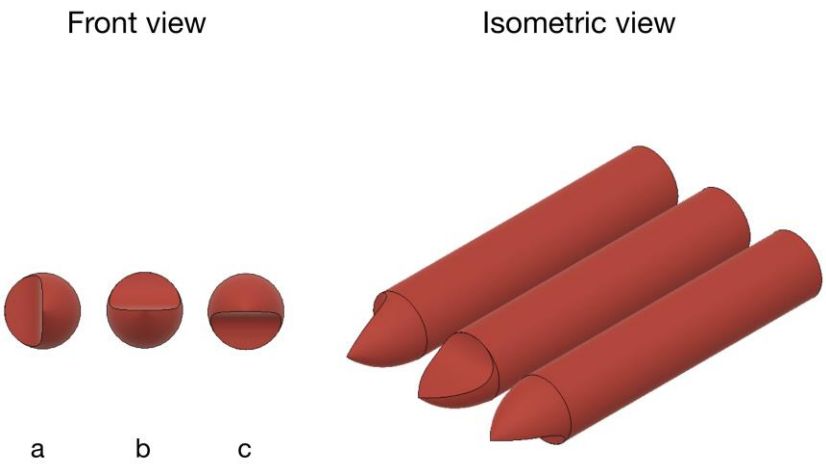

Figure 10: Front and isometric view of different orientation of asymmetric tip

As seen from the figure, (a) 'tip facing to the side' , (b) 'tip facing down', and (c) 'tip facing up'.

Summing up, just like in vertical penetration tests, the measured results are:

- Penetration resistance (q_c): The resistance against the tip as it penetrates the soil.
- Penetration advancement (d): The length the penetrometer advances into the soil.

The parameters are:

- Tip geometry
- Depth (static stress)
- Tip orientation (just for asymmetric tip)

4.2. Results

This section presents the findings from a series of experiments designed to evaluate the performance of different tip geometries during penetration tests under various conditions. The primary objective was to identify which tip shape exhibits the lowest penetration resistance, thereby optimizing the design and functionality of the soil intruding robot. The experiments were conducted across at differing densities and penetration rates to cover a broad range of scenarios. The results are grouped by tip geometry, density, penetration rate, and also by penetration advancement to get a quick overview of a combination of all tip geometry and densities.

4.2.1. Impact of Sand Density on Penetration

The graph in Figure 11 shows the relationship between penetration resistance and penetration depth for all densities.

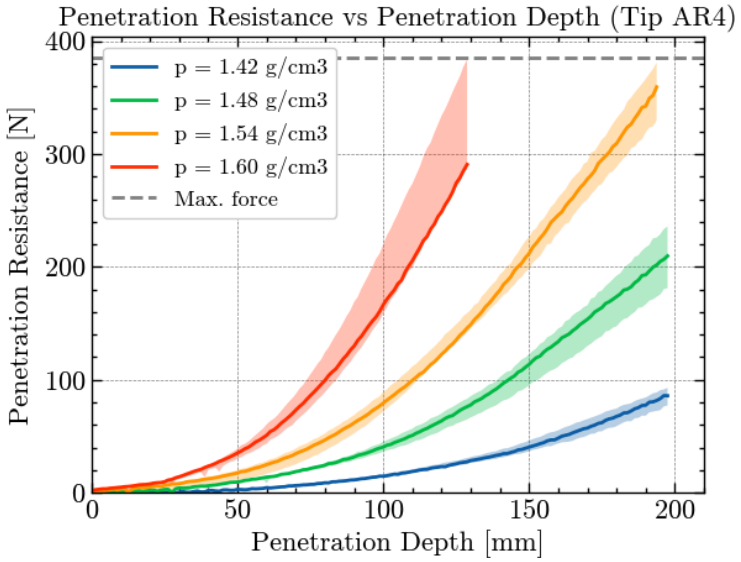

Figure 11: Penetration Resistance vs Penetration Depth plotted showing correlation with sand density of tip AR4, densities indicated in the legend

A clear correlation can be seen in the graph showing the relationship between penetration resistance and sand density. As sand density increases, penetration resistance likewise rises. Although the degree of resistance varies depending on the particular tip geometry, this trend holds true for all tested tip shapes.

4.2.2. Comparing Tip Geometries (Vertical Penetration)

In the graph in Figure 12 three different tips with varying aspect ratios are shown; AR1, AR2.5, and AR4. They present a compelling inverse relationship. As the aspect ratio of the tips increases, the penetration resistance decreases. This pattern is consistent across all tests conducted under different soil conditions.

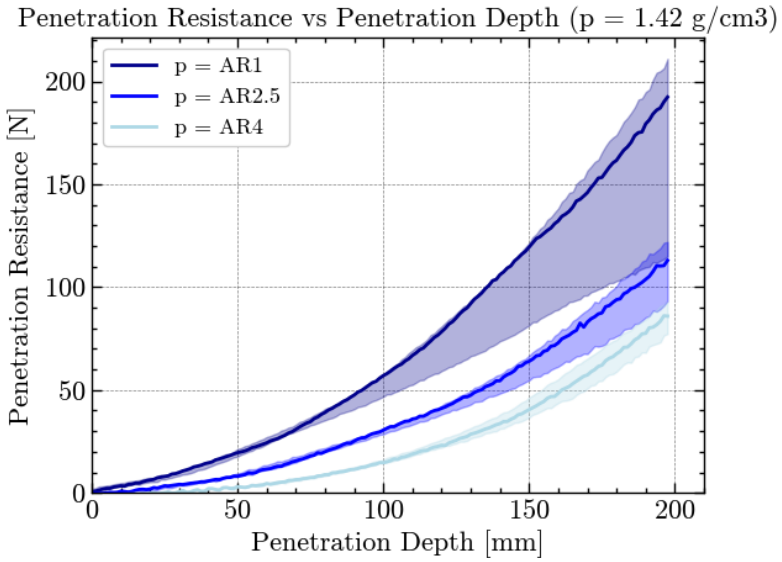

Figure 12: Penetration Resistance vs Depth showing relation with tip aspect ratio in sand bulk density p = 1.42 g/cm3, tip aspect ratio indicated in the legend

The reduction in penetration resistance with higher aspect ratios can be explained by the geometry of the tips. Tips with a higher aspect ratio are more elongated and pointed, which allows them to pierce through the sand more effectively.

In the next graph in Figure 13, the other tip shapes are included. Notably, together with AR4, the tip with the smallest diameter SD, demonstrate superior performance compared to other tested tip geometries.

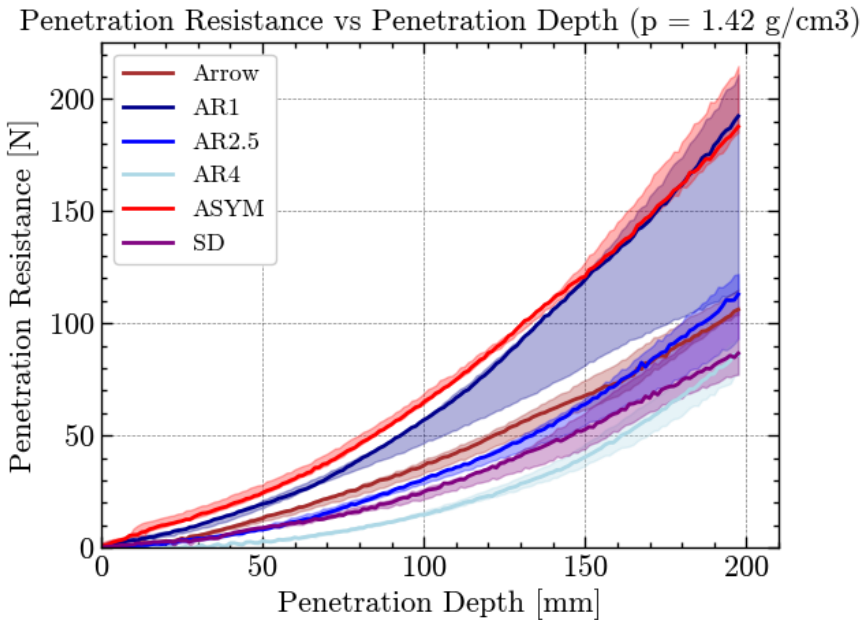

Figure 13: Penetration Resistance vs Depth for all tip geometries in sand bulk density p = 1.42 g/cm3, tip shape indicated in the legend

The results of the tip body with the smallest diameter can be attributed to the reduced surface area in contact with the sand, which decreases the friction opposing the tip's penetration. Thus smaller diameter tip bodies require less force to push through the sand.

Similarly, the tip with an aspect ratio 4, being the sharpest among the tested tip geometries, also shows excellent performance. As mentioned before, the sharp tip easily goes through the sand, minimizing the resistance encountered during penetration. However, the explanation of the good performance of a small diameter also holds for the this tip shape. The sharp, narrow tip reduces the contact area with the soil. Like the small diameter body, this minimized contact area reduces the soil's resistance against the tip's intrusion, thereby penetrating easier.

Although both AR4 and SD perform well, it can be seen that SD still experiences significantly less resistance. This pattern changes as the density of the sand is increased.

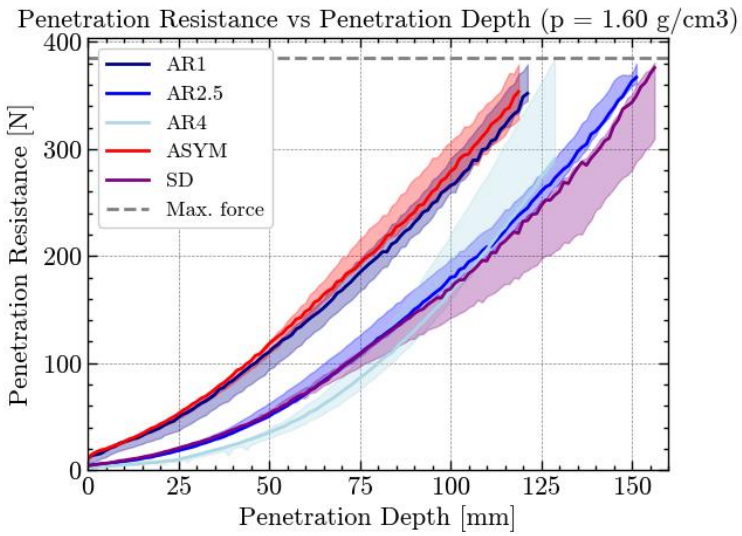

Figure 14: Penetration Resistance vs Depth in sand bulk density p = 1.60 g/cm3, tip shape indicated in the legend

In the graph shown in Figure 14, it can be seen that AR4 has the best performance due to its low penetration resistance, especially before a penetration depth of a 100 mm. After the 100 mm mark that drastically changes with SD performing better. This can be explained by the fact that after 100 mm, the base of AR4 that is 30 mm in diameter has reached the sand, thus increasing the contact area with the sand which leads to more friction on the body. This same pattern is visualized in a combined 'Force-Density' graph in Figure 15 as well. In Figure 15a, the penetration resistance at a depth of 90 mm can be seen and at a depth of 120 mm in Figure 15b. It is clear that in a lower depth (90 mm) where the only the narrow tip of AR4 is in contact with the sand, it is performing well along with tip SD. However, at a higher depth of 120 mm, tip SD has the lowest penetration resistance among all densities except for the lowest density.

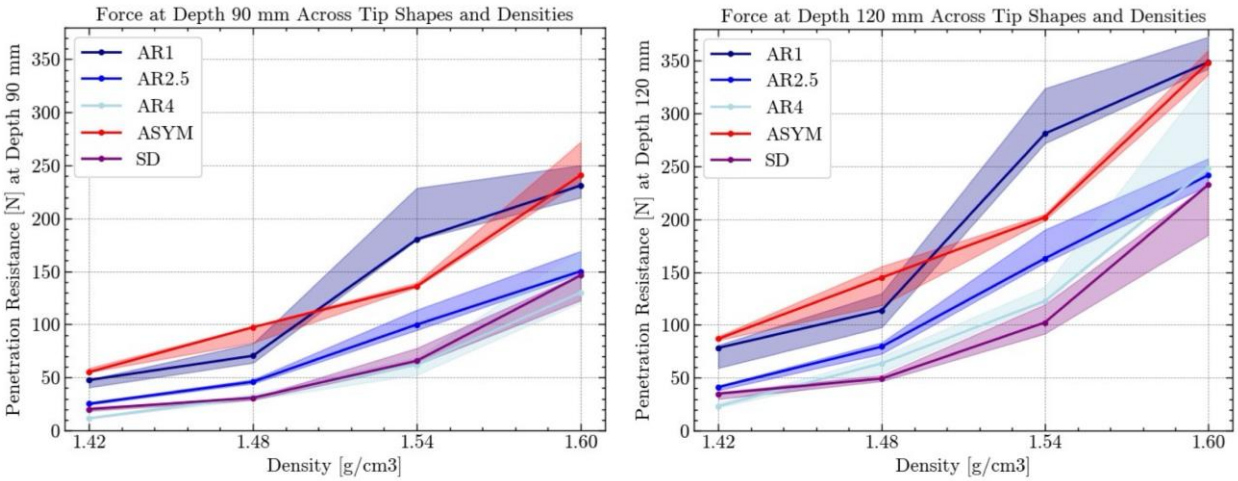

Figure 15a, b: Tip Shape - Density plot showing Penetration Resistance at depth 90 mm (a) and 120 mm (b)

Additionally, in high density conditions tip AR2.5 is performing similarly to AR4 and SD. This is again explainable by its narrow, sharp tip which goes the sand easily. On the other hand, there are tips AR1 and ASYM. Both the AR1 tip and the asymmetric tip, which share a 1:1 aspect ratio, exhibited significantly higher penetration resistance compared to other tip shapes. The equal height-to-diameter ratio (1:1) of these tips results in a blunter tip compared to tips with higher aspect ratios. This blunter geometry increases the surface area in contact with the soil at the point of entry, leading to increased friction and resistance.

The asymmetric tip, despite sharing the 1:1 aspect ratio, introduces additional challenges. Its uneven shape can cause irregular force distribution during penetration, leading to increased resistance and bending.

4.2.3. Penetration Rate

In Figure 16, multiple graphs can be seen, displaying the penetration resistance experienced by different penetration rates. Nine distinct scenarios are displayed, combining three different tip shapes with three varying soil densities, tested across three penetration rates: 1.25 mm/s, 2.5 mm/s, and 5 mm/s. Across all tested combinations of tip shapes and soil densities, the graphs consistently show negligible differences in penetration resistance as a function of penetration rate. The penetration resistance values remain broadly consistent regardless of the penetration rate being low (1.25 mm/s), medium (2.5 mm/s), or high (5 mm/s).

While the penetration resistance at 2.5 mm/s was generally lower compared to other rates (1.25 mm/s and 5 mm/s), these results may not accurately reflect the impact of penetration rate alone. This difference is more likely due to the mechanics of the setup. They could be skewed by the different initial conditions of the setup.

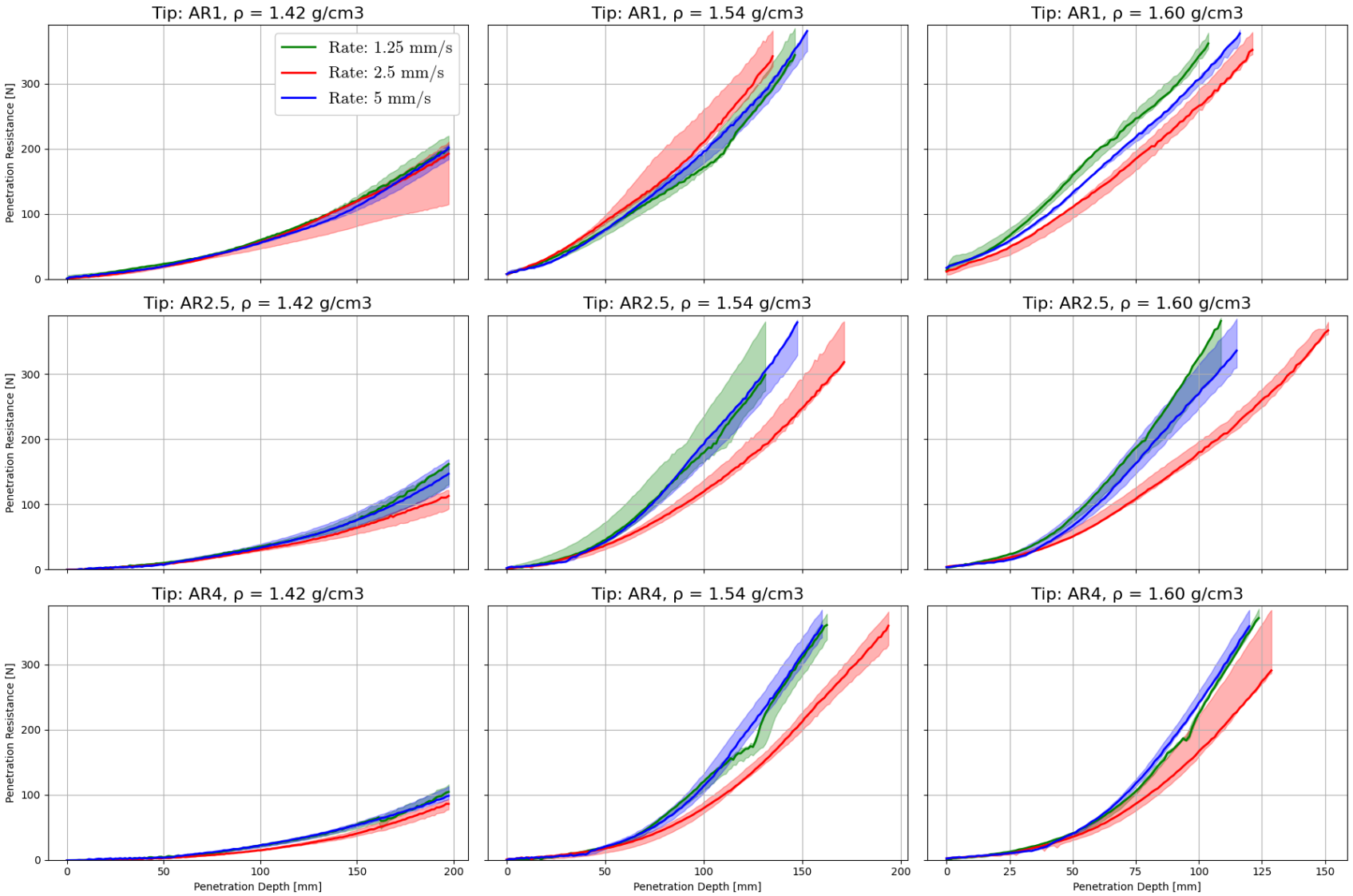

Figure 16: Penetration Resistance vs Depth showing impact of penetration rate for combinations of various tip shapes and sand densities

4.2.4. Impact of Geostatic Stress on Penetration

The results from horizontal penetration experiments reveal a clear trend: as the penetration depth (measured vertically from the surface) increases, the penetration resistance also increases. In the graph in Figure 17 this can be seen for tip AR4, where the penetration resistance is plotted against the horizontal advancement at three different depths. The deeper the penetration test is conducted, the more penetration resistance is needed. This trend is consistent among all tip shapes.

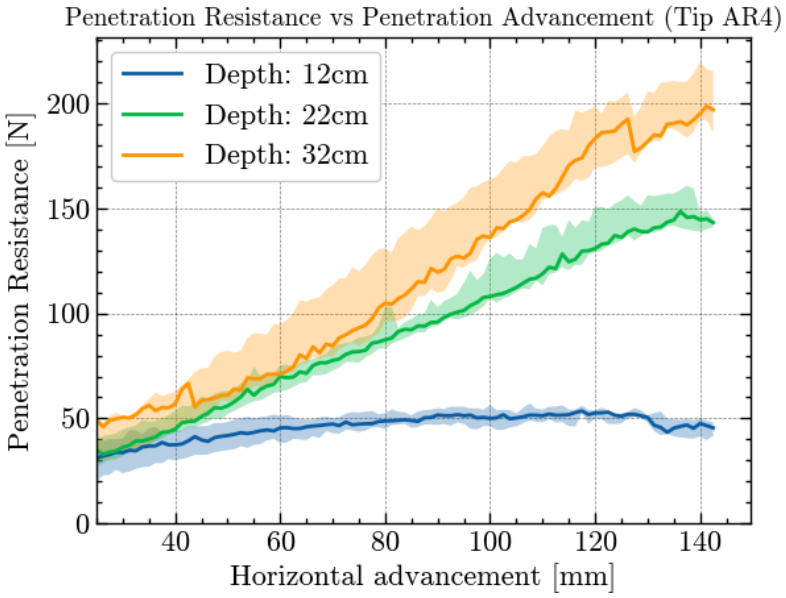

Figure 17: Penetration Resistance vs Advancement showing relation with vertical depth with tip AR4, vertical depth indicated in the legend

The primary factor contributing to increased penetration resistance at greater depths is the stress exerted by the sand above the point of penetration. As depth increases, so does the weight of the sand above the penetration site. This added stress from the overlying sand layers enhances the geostatic stress on the soil surrounding the body, thereby increasing the resistance against penetration.

4.2.5. Comparing Tip Geometries (Horizontal Penetration)

In the graph in Figure 18, the penetration resistance against horizontal advancement for multiple tip shapes is plotted. The graph illustrates that, at low depths, penetration resistance across different tip shapes remains relatively consistent, with the asymmetric tip showing a slight advantage. This could suggest that at lesser depths, the influence of tip geometry on penetration resistance is irrelevant due to lower sand compaction.

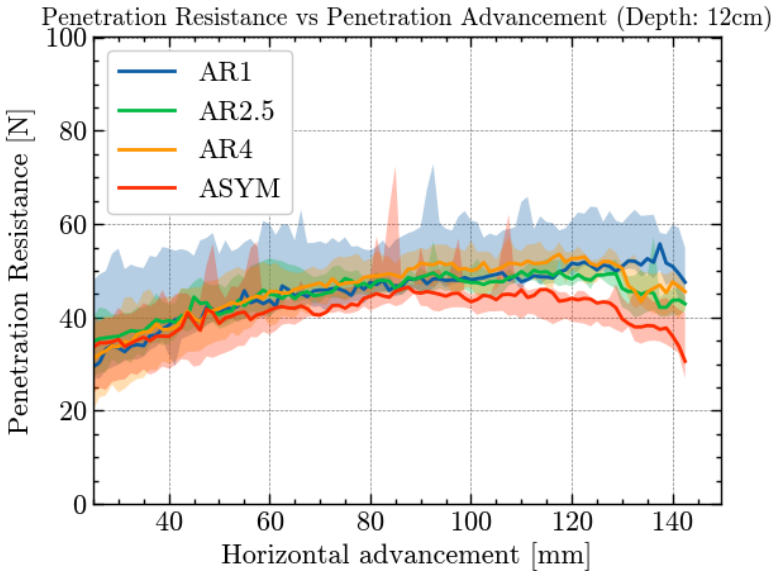

Figure 18: Penetration Resistance vs Horizontal Advancement comparing tip shapes 12 cm deep, tip shape indicated in the legend

The graph of penetration resistance at greater depths in Figure 19 reveals a notable shift in tip performance compared to shallow depths. The graph clearly illustrates that the tip with an aspect ratio of 2.5 yields the best results, surpassing even the higher aspect ratio of 4 , which is an unexpected finding. Meanwhile, the asymmetric tip has the poorest performance among the tested shapes.

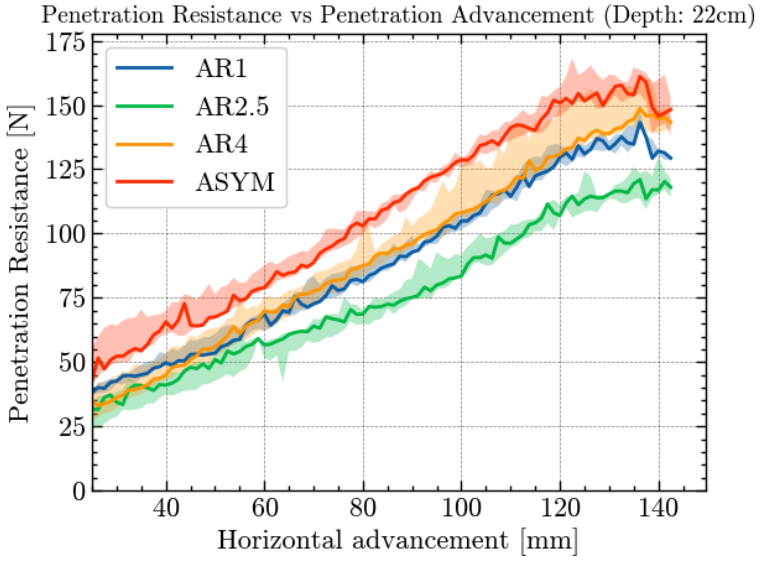

Figure 19: Penetration Resistance vs Horizontal Advancement comparing tip shapes 22 cm deep, tip shape indicated in the legend

The graph in Figure 20 gives insights into the effectiveness of different tip geometries at a high depth. The graph shows that the tip with an aspect ratio of 4 excels far beyond its counterparts,

while the asymmetric tip also performs commendably. In contrast, the tips with aspect ratios of 1 and 2.5 do not manage to reach the full penetration depth, as they exceed the maximum force (350 N).

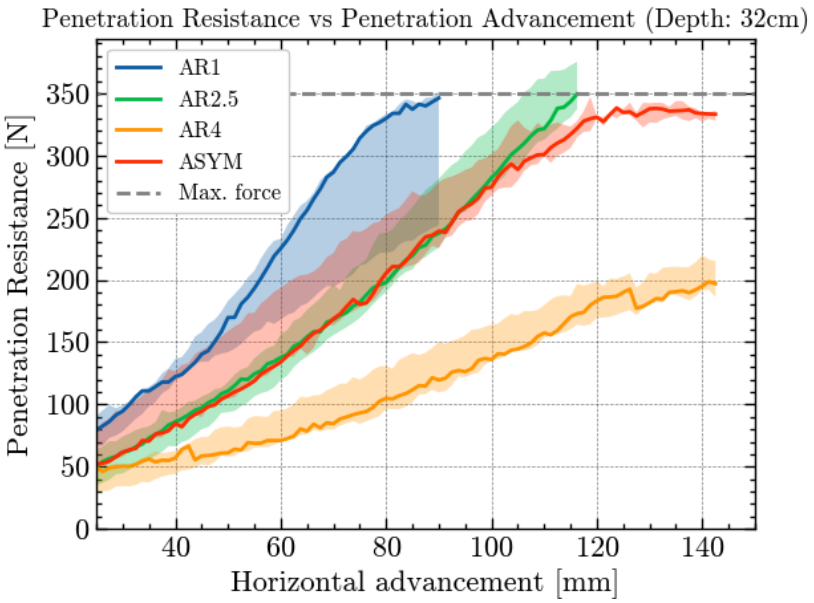

Figure 20: Penetration Resistance vs Horizontal Advancement comparing tip shapes 32 cm deep, tip shape indicated in the legend

Surprisingly, the asymmetric tip performs relatively well despite its uneven shape. This might suggest that certain asymmetrical features could be beneficial under specific soil conditions or depths, possibly by stabilizing the direction of penetration.

To further investigate the asymmetrical tip, various orientation that can be seen in Figure 10 are tested to ultimately find the most efficient orientation.

The graph in Figure 21 shows the penetration resistance for each orientation, showing a noticeable increase in resistance for the side-facing orientation, performing similarly to the tip with aspect ratio 1. As expected, the beak facing up performs well, however the beak facing down does a similar job. Ultimately, all orientations together with tip AR1 experience roughly the same resistance.

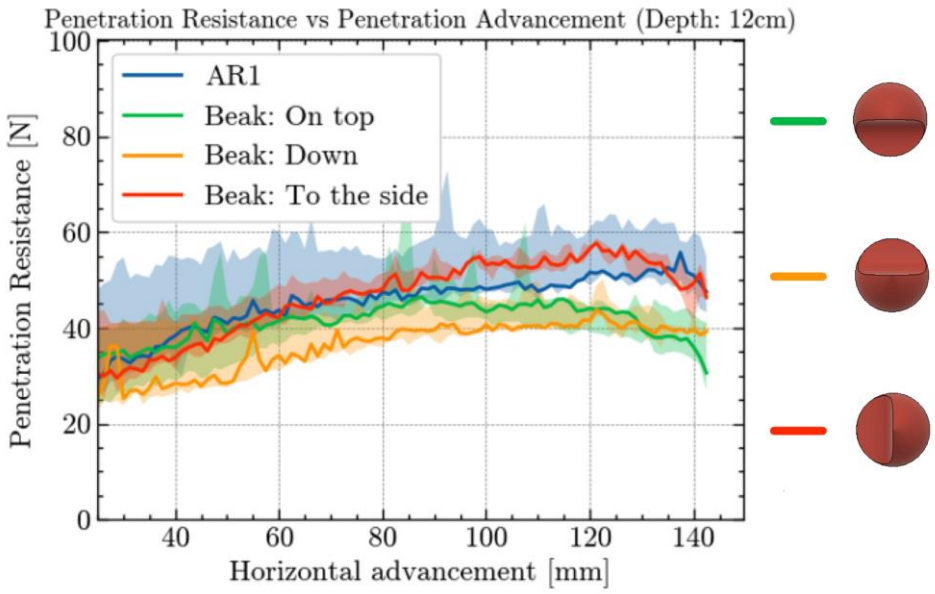

Figure 21: Penetration Resistance vs Horizontal Advancement comparing orientations of asymmetric tip and tip AR1 12 cm deep, tip shape and orientation indicated in the legend along with orientation of the tips shown on the right

5. Cavity Expansion Test

Cavity expansion testing is chosen to collect data on the interactions with the expandable chambers of the soil-intruding robot and the soil. The main parameters that are looked at during this test are the pressure applied to the chamber and the stress of the soil on the chamber.

5.1. Methodology

The cavity expansion tests will be conducted using a controlled piece of equipment designed to simulate the radial expansion of a cavity within the soil, mimicking the stress conditions generated by burrowing actions similar to those of the soil-burrowing soft robot. The equipment consists of a cylindrical chamber that can expand radially at controlled rates via connection to an external hydraulic pump. In this test the chamber will be designed using a balloon-like material. The balloon will expand radially at a predetermined rate, carefully chosen to mimic the penetration rates of soft robotic components into the soil. An example of a set up of a cavity expansion test can be seen in Figure 22.

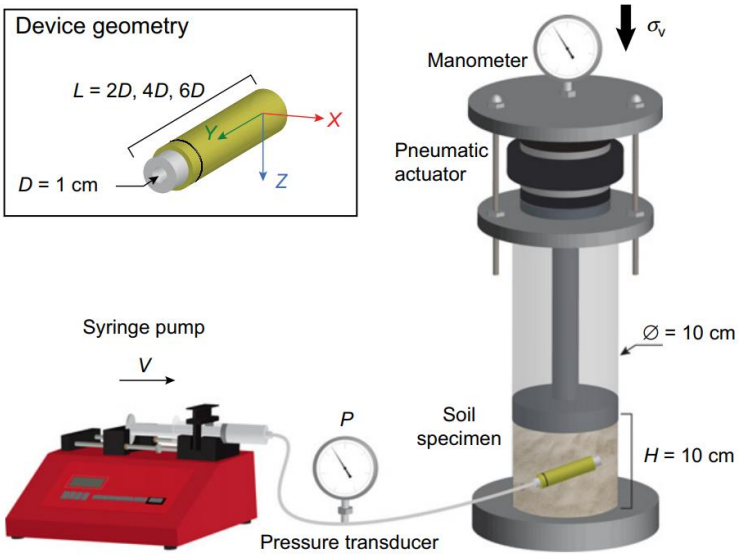

Figure 22: Example of a Set up for Cavity Expansion Test (Patino-Ramirez et al., 2023)

The radially expandable chamber can be seen in Figure 22, illustrated as the yellow cylinder. It is connected by a tube to the hydraulic pump seen in red. The manometer measures the pressure applied in the chamber.

The parameters that will be measured during the experiment are the following:

- Radial displacement of the cavity wall.
- Pressure applied to achieve radial expansion.
- Stress around the chamber.

Just like the CPT, the cavity expansion test will be performed in different soil conditions and using different chambers that differ in length and expand either isotropic or radially. Differences in length can result in different pressure, as shorter cavities show higher pressure as a result of increased volume (Patino-Ramirez et al., 2023). The different outcomes are the reason why it will be tested, as the outcome might be relevant for the robotic probe.

5.1.1. Expected Setup

Due to time constrains, the actual experiment has not been done. However, the expected setup can be seen in Figure 23.

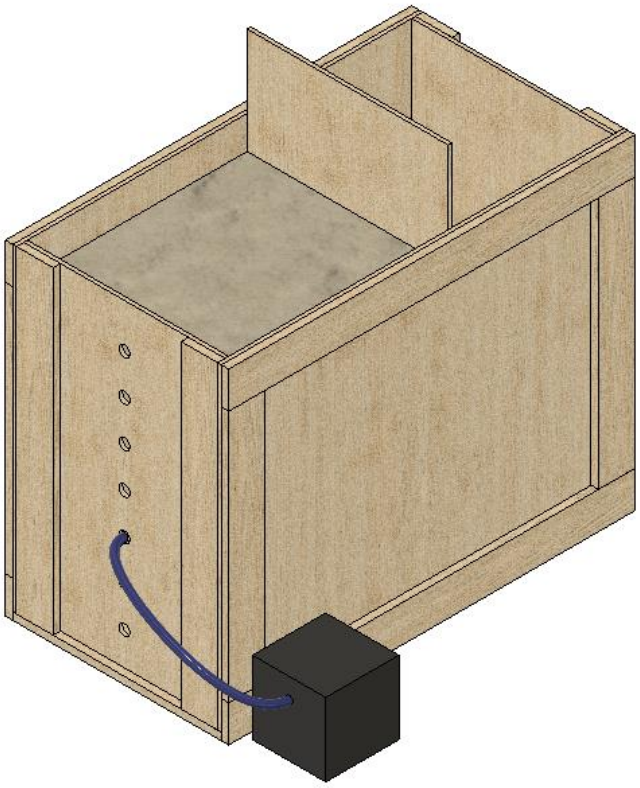

Figure 23: Expected setup for cavity expansion test, water pump illustrated as black box

The tank used for horizontal penetration is also used for the cavity expansion tests. This is because the great volume assures good results, where certain boundary conditions will not affect the tests. The chamber that will be inside the wooden tank will be filled with water. Therefore it is connected with tubes to the water pump, shown as a black box. The tubes through the holes of the corresponding depth of the chamber to minimize the length of the tubes.

6. Discussion

Several experiments were conducted to test the effectiveness of various tip shapes in soil penetration. While the data gathered has provided valuable insights, there are limitations and potential inaccuracies that must be acknowledged. These factors could have influenced the results, impacting the overall conclusions and their application in the design of the tip of the intruding robot.

One significant issue observed during the testing was the occasional bending of the tip body due to insufficiently rigid connections in the experimental setup. This mechanical instability likely affected the penetration resistance measurements. When the tip body bends, which happens due to an overload of stress on the experimental setup, not only does it alter the angle of penetration, but it also changes the dynamics of how the tip body interacts with the sand. Such bending can reduce the effective penetration force, leading to an underestimation of the soil resistance encountered by a properly aligned tip. Moreover, if bending occurred variably across different tests, it could have introduced inconsistencies in data collection, making it difficult to compare results directly across different tip shapes.

The conditions of the sand or the setup used in the tests can also significantly influence penetration resistance. If these conditions were not perfectly controlled or replicated across all tests, this would introduce another layer of variability to the results. For instance, getting to the same density multiple times, or mounting the frame to the exact same position is a task that cannot be fully controlled, and thus alter the results.

7. Recommendation

The occasional bending observed in the tip body connections during these tests highlighted a critical area for improvement. In order to improve the accuracy and consistency of upcoming experimental results, several improvements should be made.

Firstly, it is essential to modify the design of the experimental setup to ensure that all connections with the tip body are completely rigid. This can be achieved by using stronger materials for all components that connect the tip body to the penetrometer. More importantly, the threaded connections should be better. Other fastening techniques such as locking mechanisms should also be adopted to secure the tip body attachments firmly, preventing any movement or bending during penetration tests that could skew the results.

Once these enhancements are made to the rigidity of the setup, it is advisable to replicate previously conducted tests where bending was observed. This will validate the impact of the modifications on the test outcomes and ensure consistency with previous data. With a more reliable setup, it would also be feasible to expand the range of test parameters to include higher force loads or deeper penetration depths, which were previously not possible due to structural limitations. Finally, keeping detailed records of all design changes, the materials used, and the techniques implemented to enhance rigidity is essential. This documentation will not only be helpful for future experiments but can also serve as a standard protocol for similar research.

8. Conclusion

This thesis has effectively explored the impact of various tip shapes on soil penetration resistance, revealing several crucial insights that enhance our understanding of soil intruding. Through detailed experimental analysis, it has been established that tips with higher aspect ratios consistently demonstrate lower penetration resistance, especially in deeper soil layers. This reflects the advantage of sharper bodies which reduce contact area and friction against the soil, thereby facilitating easier penetration.

Additionally, the experiments highlighted the superior performance of bodies with smaller diameters, particularly noteworthy when penetrating beyond 10 cm in high-density soils (>1.54 g/cm^3). In such scenarios, the small diameter body SD outperformed even the AR4 body, suggesting that their reduced surface area becomes increasingly beneficial against deeper and more dense sand. However, the findings also showed the performance of tips in different testing orientations. While the asymmetrical body underperformed in vertical penetration tests, they excelled in horizontal tests when the beak was oriented upwards or downwards. This directional efficiency emphasizes how crucial it is to align asymmetrical features vertically in order to improve penetration stability.

One of the more surprising findings was the small influence of penetration rate on resistance, indicating that within the tested speeds, penetration efficiency is largely unaffected by the rate of advancement. This implies that optimizing tip geometry and orientation, as opposed to modifying penetration speed, might be a better emphasis for the design of the soil-intruding robot.

9. References

Broere, W., & Van Deen, J. (1998). Horizontal Cone Penetration Testing. *Geotechnical Site Characterization*.

Chowdhury, A., Ansari, S., & Bhaumik, S. (2017). Earthworm like modular robot using active surface gripping mechanism for peristaltic locomotion. *Semantic Scholar*. https://doi.org/10.1145/3132446.3134918

Dang, H. K., & Meguid, M. A. (2011). An efficient finite–discrete element method for quasi-static nonlinear soil–structure interaction problems. *International Journal for Numerical and Analytical Methods in Geomechanics*, *37*(2), 130–149. https://doi.org/10.1002/nag.1089

Huang, M., Ninić, J., & Zhang, Q. (2022). Digital Twin for underground stations : Improving decision making for construction lifecycle. *Australian Geomechanics*, *57*(3), 139–149. https://doi.org/10.56295/agj5737

Isaka, K., Tsumura, K., Watanabe, T., Toyama, W., Sugesawa, M., Yamada, Y., Yoshida, H., & Nakamura, T. (2019). Development of underwater drilling robot based on earthworm locomotion. *IEEE Access*, *7*, 103127–103141. https://doi.org/10.1109/access.2019.2930994

Lunne, T., Robertson, P. K., & Powell, J. J. M. (2002). Cone penetration testing in geotechnical practice. In *CRC Press eBooks*. https://doi.org/10.1201/9781482295047

Meurer, K., Barron, J., Chenu, C., Coucheney, E., Fielding, M., Hallett, P. D., Herrmann, A. M., Keller, T., Koestel, J., Larsbo, M., Lewan, E., Or, D., Parsons, D., Parvin, N., Taylor, A., Vereecken, H., & Jarvis, N. (2020). A framework for modelling soil structure dynamics induced by biological activity. *Global Change Biology*, *26*(10), 5382–5403. https://doi.org/10.1111/gcb.15289

Omori, H., Nakamura, T., & Yada, T. (2009). An underground explorer robot based on peristaltic crawling of earthworms. *Industrial Robot*, *36*(4), 358–364. https://doi.org/10.1108/01439910910957129

Patino-Ramirez, F., Anselmucci, F., Andò, E., Viggiani, G., Caicedo, B., & Arson, C. (2023). Deformation and failure mechanisms of granular soil around pressurised shallow cavities. *Geotechnique*, *73*(3), 265–280. https://doi.org/10.1680/jgeot.21.00136

Schmertmann, J. H. (1978). GUIDELINES FOR CONE PENETRATION TEST. (PERFORMANCE AND DESIGN). *Rosap*. https://rosap.ntl.bts.gov/view/dot/958/dot_958_DS1.pdf

Winstone, B., Pipe, A. G., Melhuish, C., Callaway, M., Etoundi, A. C., & Dogramadzi, S. (2016). Single motor actuated peristaltic wave generator for a soft bodied worm robot. *IEEE*. https://doi.org/10.1109/biorob.2016.7523668